

This article was downloaded by: [University of Southampton]

On: 26 May 2010

Access details: Access Details: [subscription number 908420906]

Publisher Taylor & Francis

Informa Ltd Registered in England and Wales Registered Number: 1072954 Registered office: Mortimer House, 37-41 Mortimer Street, London W1T 3JH, UK



Combustion Theory and Modelling

Publication details, including instructions for authors and subscription information:

<http://www.informaworld.com/smpp/title~content=t713665226>

The effect of oxygen starvation on ignition phenomena in a reactive solid containing a hot-spot

A. Shah^{ab}; A. McIntosh^b; J. Brindley^a; J. Griffiths^c; M. Pourkashanian^b

^a Department of Applied Mathematics, University of Leeds, Leeds, UK ^b Department of Fuel and Energy, University of Leeds, Leeds, UK ^c Department of Chemistry, University of Leeds, Leeds, UK

Online publication date: 17 July 2003

To cite this Article Shah, A. , McIntosh, A. , Brindley, J. , Griffiths, J. and Pourkashanian, M.(2003) 'The effect of oxygen starvation on ignition phenomena in a reactive solid containing a hot-spot', Combustion Theory and Modelling, 7: 3, 509 – 523

To link to this Article: DOI: 10.1088/1364-7830/7/3/304

URL: <http://dx.doi.org/10.1088/1364-7830/7/3/304>

PLEASE SCROLL DOWN FOR ARTICLE

Full terms and conditions of use: <http://www.informaworld.com/terms-and-conditions-of-access.pdf>

This article may be used for research, teaching and private study purposes. Any substantial or systematic reproduction, re-distribution, re-selling, loan or sub-licensing, systematic supply or distribution in any form to anyone is expressly forbidden.

The publisher does not give any warranty express or implied or make any representation that the contents will be complete or accurate or up to date. The accuracy of any instructions, formulae and drug doses should be independently verified with primary sources. The publisher shall not be liable for any loss, actions, claims, proceedings, demand or costs or damages whatsoever or howsoever caused arising directly or indirectly in connection with or arising out of the use of this material.

The effect of oxygen starvation on ignition phenomena in a reactive solid containing a hot-spot

A Shah^{1,2}, A McIntosh², J Brindley¹, J Griffiths³ and M Pourkashanian²

¹ Department of Applied Mathematics, University of Leeds, Leeds LS2 9JT, UK

² Department of Fuel and Energy, University of Leeds, Leeds LS2 9JT, UK

³ Department of Chemistry, University of Leeds, Leeds LS2 9JT, UK

Received 6 December 2002, in final form 23 April 2003

Published 17 July 2003

Online at stacks.iop.org/CTM/7/509

Abstract

In this paper, we explore the effect of oxygen supply on the conditions necessary to sustain a self-propagating front from a spherical source of heat embedded in a much larger volume of solid. The ignition characteristics for a spherical hot-spot are investigated, where the reaction is limited by oxygen, that is, reactant + oxygen \rightarrow product. It is found that over a wide range of realistic oxygen supply levels, constant heating of the solid by the hot-spot results in a self-propagating combustion front above a certain critical hot-spot power; this is clearly an important issue for industries in which hazard prevention is important. The ignition event leading to the formation of this combustion wave involves an extremely sensitive balance between the heat generated by the chemical reaction and the depletion of the reactant. As a result, for small hot-spot radii and infinite oxygen supply, not only is there a critical power above which a self-sustained combustion front is initiated there also exists a power beyond which no front is formed, before a second higher critical power is found. The plot of critical power against hot-spot radius thus takes on a Z-shape appearance. The corresponding shape for the oxygen-limited reaction is qualitatively the same when the ratio of solid thermal diffusion to oxygen mass diffusion (N) is small and we establish critical conditions for the initiation of a self-sustained combustion front in that case. As N gets larger, while still below unity, we show that the Z-shape flattens out. At still larger values of N , the supercritical behaviour becomes increasingly difficult to define and is supplanted by burning that depends more uniformly on power. In other words, the transition from slow burning to complete combustion seen at small values of N for some critical power disappears. Even higher values of N lead to less solid burning at fixed values of power.

1. Introduction

Recent works, reported by Brindley *et al* [1–3], have studied the effect of a constant source of heat on a reactive solid X, where the reaction was assumed to be of the form



In this paper, we extend this work by introducing an oxidant O into the reaction scheme



which is required to diffuse into the porous matrix of the solid X. The background and partly the motivation for this, as in the original studies [1–3], is the exothermic degradation and subsequent ignition of combustible solids such as bulk powders and coal dust (occurring, e.g. in many operations in the process control industry) if they are inadvertently exposed to thermal energy. Equipment such as blenders, mills and screw feeders can develop localized heat sources from mechanical impact or failure of a component such as a bearing. Power cables that have suffered local damage may also be a source. The source of heat, or ‘hot-spot’, would almost invariably cause local destruction through slow local combustion, and one issue is the extent to which the degradation penetrates the surrounding material. Alternatively, it may initiate a self-propagating combustion wave (which implies virtually total loss of the product) and possibly lead to some greater catastrophe such as fire or explosion. Clearly, an understanding of the conditions under which thermal decomposition occurs and the extent of the decomposition are crucial in hazard prevention. More generally, we are interested in understanding the ignition, intended or otherwise, of reactive solids by nearby heating sources and its dependence on a limited oxygen supply.

Some of the issues mentioned above have been considered previously. For example, in [4, 12], the authors focus on predicting the critical initial conditions for the safe storage of potentially exothermic materials; a study of spontaneous ignition. On the other hand, the characteristics and properties of a fully developed combustion wave have been addressed in, amongst others [5, 9, 10]. In this paper, we are concerned primarily with the criteria for the onset of ignition, with particular emphasis on low exothermicity materials and in circumstances in which the ingress of oxygen may be restricted.

Analytical progress in describing the ignition event using the equation in [1] has proved to be far from straightforward, even in the simpler model. Although first Linan and Williams [7], and then Kapila [6] (see also [11]), have developed an asymptotic theory for the ignition of a solid subjected to a constant heat flux, they have done so either without reactant consumption (the former) or by inferring results from the gaseous case (the latter), and in both cases the geometry was planar. The presence of reactant consumption and the spherical geometry introduce further significant complications.

Both size and shape are of particular significance in this problem, and in an earlier work [2] we have established that full non-dimensionalization is not viable. However, the dynamics of development of combustion are such that, beyond a certain condition, there is little sensitivity to the outer boundary, but it is necessary to define the absolute size of the hot-spot.

In this paper, we are stressing the three-dimensionality of the system that is simply represented by the spherical geometries of both the hot-spot and the reactant mass. We believe that all sufficiently large three-dimensional volumes will exhibit the behaviour discussed in [1] and illustrated in figure 1. The effect of the distant boundary is not felt in the initial stages. Experimental evidence suggests that in cubes of non-spherical form, the evolution from an internal hot-spot shows a strong degree of spherical symmetry.

For simplicity, and as in [1], we assume that both the reactant material and the hot-spot are spherical, the latter placed at the centre of the former, and that the fully burnt material

occupies the same volume and has the same characteristics as the unburnt material. The latter assumption is important to this work. We are assuming that there is no change of phase and that the product is a solid of a similar density to that of the reactant. The surface of the hot spot, $r = r_0$, is assumed to be a constant source of heat flux \tilde{P} , with corresponding total power $p = 4\pi r_0^2 \tilde{P}$ W.

The following terminology, having originated in earlier works [1–3], is used throughout.

- A situation where a self-sustained combustion wave is initiated is termed supercritical. All other situations are termed subcritical. It will be clear from comparing examples of these two behaviours in section 3 that the two cases are readily distinguished. In particular, the supercritical behaviour leads to a self-sustained combustion front, and eventually to complete burning of the material (except for a small boundary layer near the outer surface of the fuel, for the reason explained in section 2) in a relatively short period of time (from the point of initiation of the wave). Furthermore, the evolution of the profiles for temperature and fuel density are very different.
- For a given hot-spot size r_0 , we term a region in \tilde{P} space safe if for all values of \tilde{P} in this region only the subcritical behaviour is found.

2. Mathematical model

The governing equations, assuming spherical symmetry with radial coordinate r and time τ , can be written as follows:

$$\begin{aligned} \rho C_p \frac{\partial T}{\partial \tau} - \frac{\lambda}{r^2} \frac{\partial}{\partial r} \left(r^2 \frac{\partial T}{\partial r} \right) &= Q A X Y e^{-E/RT}, \\ \frac{\partial Y}{\partial \tau} - \frac{D_Y}{r^2} \frac{\partial}{\partial r} \left(r^2 \frac{\partial Y}{\partial r} \right) &= -A X Y e^{-E/RT}, \\ \frac{\partial X}{\partial \tau} &= -A X Y e^{-E/RT}, \end{aligned} \quad (3)$$

in which T is the temperature of the solid, and X and Y are the densities of the reactant and oxygen, respectively. It is assumed that the reactant diffusion coefficient is negligibly small, as is usually the case with solids. We also assume that the heat transfer rate between the solid and the gas is sufficiently large to adopt the same temperature field for both. The other quantities appearing in (3) are defined in table 1. The boundary conditions for temperature are

$$T(r_1, \tau) = T_a, \quad (4a)$$

$$-\lambda \frac{\partial T}{\partial r}(r_0, \tau) = \tilde{P}, \quad (4b)$$

corresponding to a total heat flux \tilde{P} across the surface of the hot-spot $r = r_0$, and ambient conditions at the outer edge of the solid $r = r_1$. For the oxygen density we have

$$Y(r_1, \tau) = Y_a, \quad \frac{\partial Y}{\partial r}(r_0, \tau) = 0, \quad (5)$$

where Y_a is the initial oxygen density given in table 1.

(a) It is important to note that boundary condition (4a) means that the reaction is always very slow at the boundary $r = r_1$, so that in reality there is always a thin boundary layer of incomplete combustion near that surface. This boundary condition is commonly used in these problems and represents an infinite Biot number condition. Thus, when we refer to complete burning or complete burnout of the fuel in what follows (see also the definitions

Table 1. Values for quantities used in the calculations.

Quantity	Symbol	Value
Pre-exponential factor	A	$6.6 \times 10^7 \text{ kg}^{-1} \text{ m}^3 \text{ s}^{-1}$
Heat of reaction	Q	$5.7 \times 10^5 \text{ J kg}^{-1}$
Activation energy	E	$8.4 \times 10^7 \text{ J kmol}^{-1}$
Universal gas constant	R	$8314 \text{ J kmol}^{-1} \text{ K}^{-1}$
Fuel density	ρ	660 or 270 kg m^{-3}
Specific heat	C_p	$750 \text{ J kg}^{-1} \text{ K}^{-1}$
Thermal conductivity	λ	0.1 or $0.01 \text{ W m}^{-1} \text{ K}^{-1}$
Ambient/initial temperature	T_a	300 K
Initial oxygen density	Y_a	$0.27 \times 10^{-3} \text{ kg m}^{-3}$
Reactant radius	r_1	0.05 m
Hot-spot radius	r_0	Varied between 0.000 75 and 0.01 m
Oxygen diffusion coefficient	D_Y	Determined through N
Ratio of densities	$\beta = \rho/Y_a$	2440 or 1000

in section 1), we mean that all but a thin layer near $r = r_1$ of the fuel has been consumed. Boundary condition (4b) is the simplest boundary condition possible and we acknowledge that it is possible to have a condition in which some leakage of the oxygen into the hot-spot takes place. Finally, the initial conditions are given by

$$T(r, 0) = T_a, \quad X(r, 0) = \rho, \quad Y(r, 0) = Y_a. \quad (6)$$

We nondimensionalize the variables by rescaling as follows:

$$\begin{aligned} u &= \frac{RT}{E}, & y &= \frac{Y}{Y_a}, & x &= \frac{X}{\rho}, & \xi &= \frac{r}{r_1}, & t &= \frac{\lambda \tau}{\rho C_p r_1^2}, \\ q &= \frac{QR}{EC_p}, & a &= \frac{AY_a \rho C_p r_1^2}{\lambda}, & \beta &= \frac{\rho}{Y_a}, \\ N &= \frac{\lambda}{Y_a C_p D_Y}, & \alpha &= \frac{\tilde{P} R r_1}{\lambda E}, & u_a &= \frac{RT_a}{E}. \end{aligned} \quad (7)$$

The result of substituting (7) into (3)–(6) is

$$\begin{aligned} \frac{\partial u}{\partial t} - \frac{1}{\xi^2} \frac{\partial}{\partial \xi} \left(\xi^2 \frac{\partial u}{\partial \xi} \right) &= q a x y e^{-1/u}, \\ \frac{\partial y}{\partial t} - \frac{\beta}{N} \frac{1}{\xi^2} \frac{\partial}{\partial \xi} \left(\xi^2 \frac{\partial y}{\partial \xi} \right) &= -a \beta x y e^{-1/u}, \\ \frac{\partial x}{\partial t} &= -a x y e^{-1/u} \end{aligned} \quad (8)$$

and

$$\begin{aligned} \frac{\partial u}{\partial \xi} + \alpha &= 0, & \frac{\partial y}{\partial \xi} &= 0 & \text{at } \xi &= \xi_0, \\ u(1, t) &= u_a, & y(1, t) &= 1, \\ u(\xi, 0) &= u_a, & x(\xi, 0) &= 1, & y(\xi, 0) &= 1. \end{aligned} \quad (9)$$

2.1. Remarks concerning N and β

By choosing N small enough, the system (8) and (9) is equivalent to the one-reactant system considered [1]. Thus, we note that the oxygen equation, as $N \rightarrow 0$, is given by

$$\frac{1}{\xi^2} \frac{\partial}{\partial \xi} \left(\xi^2 \frac{\partial y}{\partial \xi} \right) = O(N) \ll 1, \quad (10)$$

when all other parameters are fixed. The solution to (10), subject to the boundary conditions, is $y = 1 + O(N)$, and thus in this important limit oxygen has a negligible effect on the calculations.

It is found that the parameters $\beta = \rho/Y_a$ and N are crucial for the calculations. We fix β at a realistic value and allow N to vary between 0 and 10. The latter value represents an upper bound on the realistic values of N , which we expect most likely to be around unity in real situations.

To calculate β we note that the density of oxygen Y_a is (from the ideal gas law) given by $W_{O_2} P_{O_2} / RT$, where W_{O_2} and P_{O_2} are the molecular mass and partial pressure of oxygen, respectively. Hence, for atmospheric pressure Y_a is 0.27 kg m^{-3} (assuming P_{O_2} is $0.21 \times 10^5 \text{ Pa}$ and W_{O_2} is 32 kg kmol^{-1}). With $\rho = 660 \text{ kg m}^{-3}$, we get $\beta \approx 2440$. However, for a lighter fuel density of 270 kg m^{-3} , we get $\beta \approx 1000$. We have performed a number of numerical experiments for $\beta = 2440$, but also include some cases of $\beta = 1000$. We have also performed a separate numerical experiment for a different value of the thermal conductivity λ , for it is important to realize that packing of powders strongly influences the effective thermal heat transfer.

The initial boundary problem was solved in Fortran using routines from the NAG Library. In the calculations, the number of grid points was typically around 2000 and the time-step varied depending on the stiffness of the finite-differenced system.

3. Results

Unless otherwise stated, we use $r_1 = 0.05 \text{ m}$. Changing r_1 did not qualitatively alter the results. Furthermore, the results are presented in dimensional form, although in future work it is planned to repeat many of the calculations in dimensionless form to study the effect of scale. This is discussed further below.

3.1. Small N

In figures 2–5, we show the values of the dimensional temperature, T , and the dimensionless values of the reactant concentrations, x and y . This makes the profiles clearer and easier to understand.

The results for small N in the oxygen-limited model (8) and (9) can be summarized in figure 1, which shows the critical values of power required to initiate self-sustained combustion against hot-spot radius. For N below 0.3, the results do not differ quantitatively from those of [1]. Consider the case $N = 0.1$. Above $r_0 \approx 0.0044 \text{ m}$ there is a well-defined cut-off between supercritical and subcritical behaviours. For $r_0 = 0.004 \text{ m}$, in the subcritical case (figure 2(a)), the oxygen mass fraction remains almost constant around unity, after $t = 5 \text{ min}$, and the degradation of the material is confined to around 0.01 m at $t = 10 \text{ min}$ (at $t = 100 \text{ min}$ the burning only reaches $r = 0.013 \text{ m}$). In contrast, at a slightly higher value of power (figure 2(b)), the temperature profiles indicate clearly that a self-sustained combustion wave has been initiated leading to complete burnout (except, as mentioned, at the outer boundary of the material).

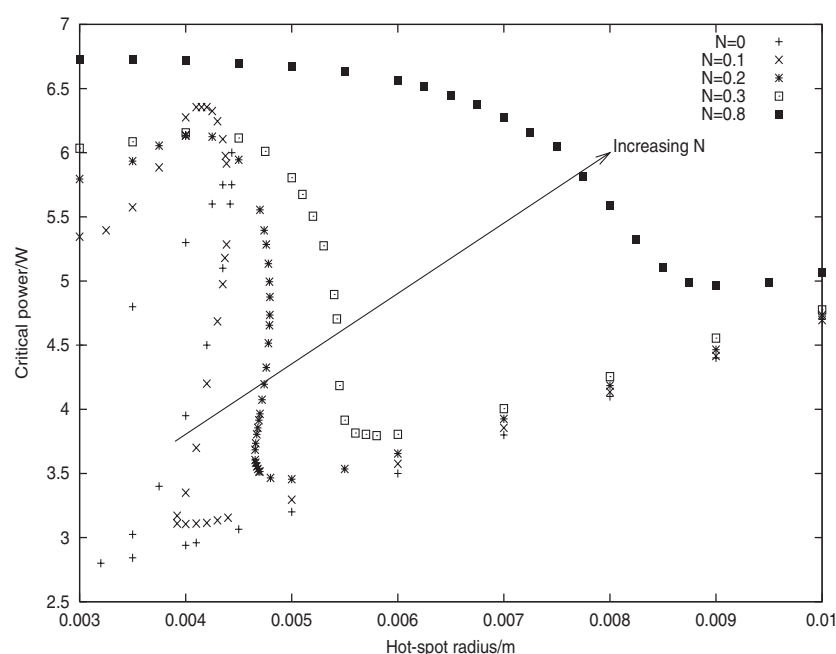


Figure 1. The critical power curves for an increasing range of N . As N is increased, the 'Z-shape' behaviour disappears. The parameter values used here are $\rho = 660 \text{ kg m}^{-3}$, $\beta = 2440$ and $\lambda = 0.1 \text{ W m}^{-1} \text{ K}^{-1}$. Compare the curve $N = 0.1$ ('x') with figure 6, where $\rho = 270 \text{ kg m}^{-3}$, $\beta = 1000$ and $\lambda = 0.1 \text{ W m}^{-1} \text{ K}^{-1}$, and figure 7, where $\rho = 660 \text{ kg m}^{-3}$, $\beta = 2440$ and $\lambda = 0.01 \text{ W m}^{-1} \text{ K}^{-1}$.

The decomposition of the reactant occurs adjacent to the heat source at the initial stages in figure 2(a), where $P = 3.1 \text{ W}$. The rate of decomposition, however, slows down significantly beyond $t \approx 3.5 \text{ min}$, which is also the time at which the temperature at the surface of the hot-spot begins to fall. Ultimately, the combustion front comes almost to a stop before the material is completely burnt through. In sharp contrast to this behaviour, at $P = 3.11 \text{ W}$ (figure 2(b)), combustion becomes self-sustained not long after $t = 3 \text{ min}$, leading to the burnout of the material. The predicted duration time for complete combustion is around 7 min (except for a small boundary layer at the edge of the material ($r = r_1$) where the boundary condition $T = T_a$ exists, so that in that small region there is always incomplete combustion). In this example, the critical power for complete combustion to occur is $3.105 \pm 0.05 \text{ W}$. If a small enough ratio N is assumed, the result would be identical to that for the one-reactant case, discussed in [1–3].

As we increase the hot-spot radius, we find that the time required to initiate the supercritical behaviour increases and the speed of the subsequent combustion wave is lower. This can be seen by comparing figure 2 with figures 3 and 4, the latter two being for $r_0 = 0.006 \text{ m}$ and $r_0 = 0.01 \text{ m}$, respectively. For $0.00385 < r_0 < 0.0044$, there exists an apparently 'safe' region between two critical powers. In this region, the subcritical behaviour prevails. However, as we increase the power within this safe region, more reactant is consumed before the burning stops. We also found instances in which the supercritical behaviour is initiated at the second or third attempt (the burning appears to accelerate for a short period only to slow down before it once again accelerates and forms a self-sustained wave—see earlier definitions of the terms 'subcritical' and 'supercritical' in section 1). This could well be related to the oscillatory burning of solids.

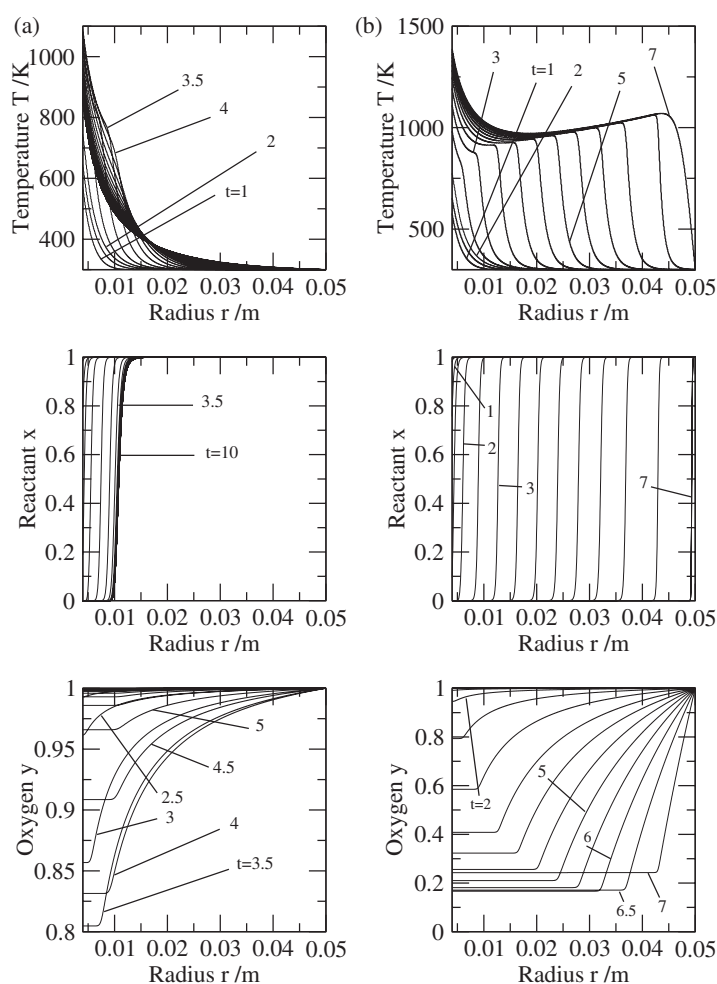


Figure 2. Subcritical behaviour (a) $P = 3.1$ W and supercritical behaviour, (b) $P = 3.11$ W for $N = 0.1$ and $r_0 = 0.004$ m. In (a) profiles are shown every 0.5 min up to $t = 10$ min and in (b) profiles are shown every 0.5 min up to $t = 7$ min.

Returning to figure 1 and comparing the critical curve for $N = 0.1$ with the one-reactant curve, we see a narrowing of the range of hot-spot radius in which the safe region appears. The narrowing of the region increases as we increase N . In addition, the curves appear to flatten out and by $N = 0.3$ we see that the safe region disappears altogether. When N reaches unity, the supercritical behaviour itself disappears (discussed later).

Increasing N , and thereby decreasing the oxygen diffusivity D_Y , makes it more difficult for the oxygen to diffuse to regions where it has depleted. This, in turn, would make it more difficult to sustain combustion. This is partly what we observe in figure 1. As we increase N , the critical curve gets higher on both sides of the region where multiple critical powers are found, indicating that a higher critical power is required for a fixed hot-spot radius. However, in the region with multiple critical powers, this trend is not followed. Furthermore, we found that for N close to unity it is no longer possible to define a critical power curve (see later). This change in behaviour is partly explained by the balance of terms in oxygen equation (8). We can predict a change in behaviour when the diffusion term (coefficient N) reaches the same order

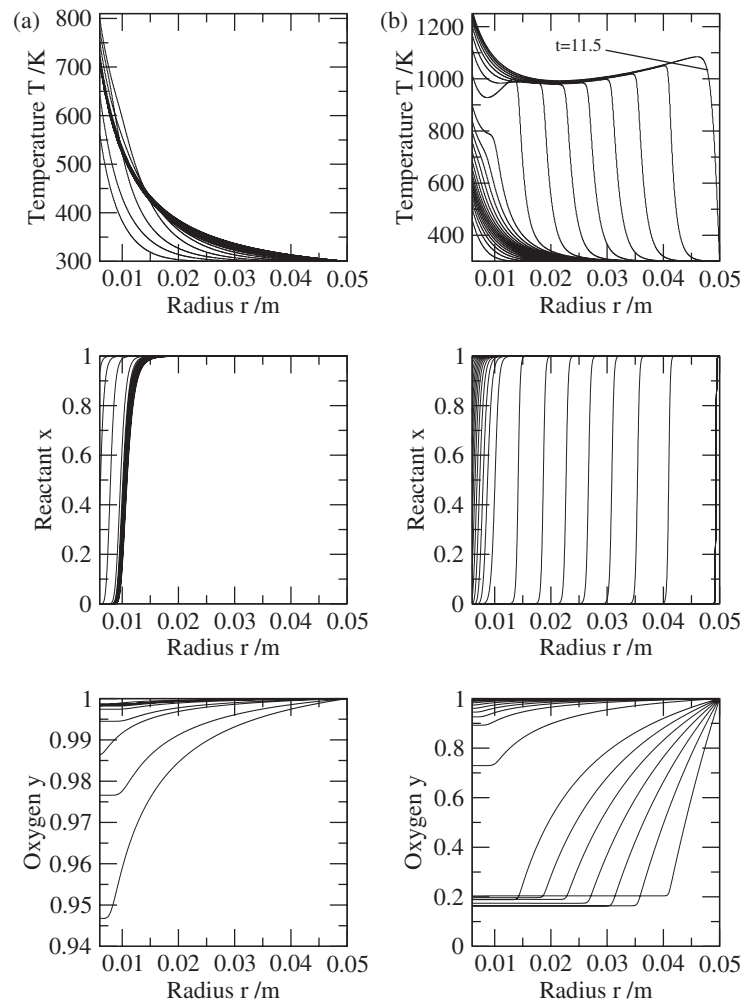


Figure 3. Subcritical behaviour (a) $P = 3.57$ W to $t = 50$ min in steps of 2.5 min and supercritical behaviour (b) $P = 3.58$ W to $t = 11.5$ min in steps of 0.5 min for $N = 0.1$ and $r_0 = 0.006$ m.

of magnitude as the reaction rate. At this point, we can expect the (increased) depletion rate of oxygen to become dominant, and thus become the reaction-rate limiting process.

Figure 1 shows that the restriction on oxygen diffusion as N increases from zero does not alter the overall character of the ignition behaviour, particularly for small r_0 . But near $N = 0.3$ the character is finally affected, in that the switch-off behaviour disappears.

3.2. N approaching unity and beyond

As N moves close to unity, it becomes more difficult to define the transitional behaviour between the sub- and supercritical behaviours seen at small N . It is likewise difficult to say where this behaviour occurs, but in both cases ($\beta = 2440$ and $\beta = 1000$) the transitional behaviour is still seen at $N = 0.9$ and not at $N = 1.1$. Consider $N = 0.9$, where the burning of the solid material is strongly controlled by the oxygen supply. For small hot-spot powers the subcritical behaviour prevails. At the critical power, it is seen that the oxygen

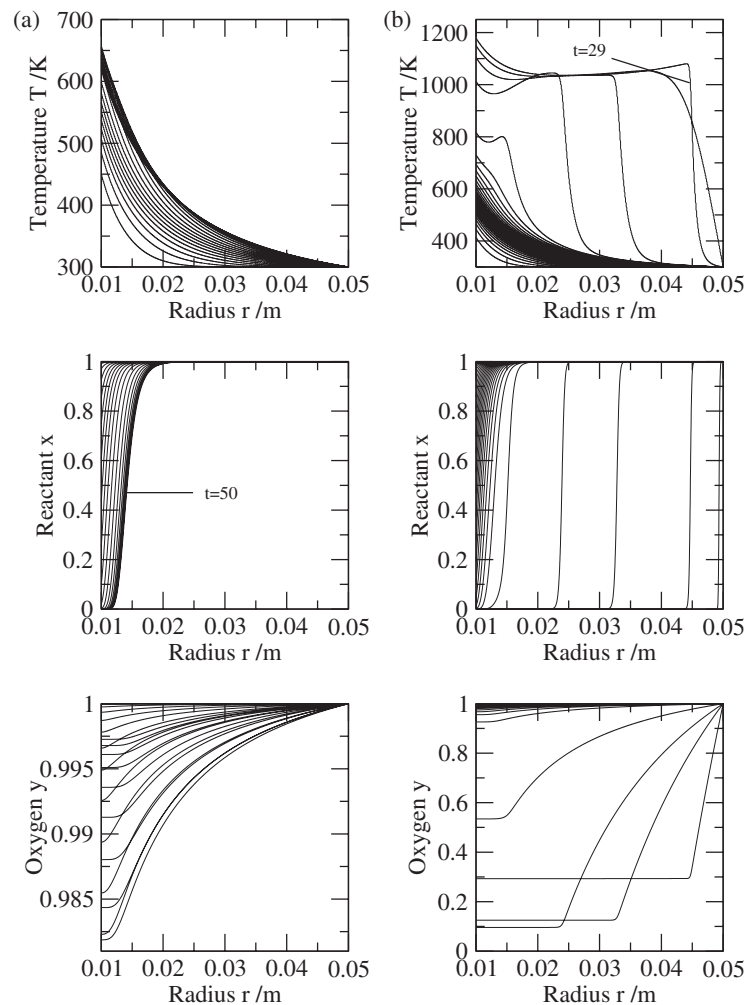


Figure 4. Subcritical behaviour (a) $P = 4.65$ W to $t = 50$ min in steps of 2.5 min and supercritical behaviour (b) $P = 4.75$ W to $t = 30$ min in steps of 1 min for $N = 0.1$ and $r_0 = 0.01$ m.

initially depletes too rapidly to sustain combustion, allowing it to diffuse back to the reaction zone from the outer boundary, at which time the reaction begins again and the burning of the solid goes to completion. In the subcritical cases, the same behaviour is seen except that the reaction is not continued when the oxygen diffuses back from the boundary. For $N > 0.9$, the 'critical' power required to bring about the burning after the oxygen diffuses back from the outer boundary becomes increasingly larger. There is, correspondingly, an increasingly smaller difference between the degree of burning for values just above and just below this 'critical' value. Therefore, it is no longer feasible to talk of transition (and a critical power) from slow burning to self-sustained complete burning. In what follows, for N close to unity, it becomes evident that the characteristics of the solutions change, such that whether the reaction is sub- or supercritical is no longer the issue, but rather the extent of burning.

For such values of N (close to unity):

- (i) an increasingly larger power is required to achieve the same degree of reactant depletion;
- (ii) self-sustained propagation is not possible;

Table 2. The depth of burnt product r_b in metre for $N = 1.2$ when the hot-spot radius is varied.

Power (W)	$r_0 = 0.01$ m	$r_0 = 0.008$ m	$r_0 = 0.006$ m	$r_0 = 0.004$ m
4	0.008 18	0.008 09	0.007 93	0.007 85
5	0.010 52	0.010 36	0.010 11	0.009 33
6	0.019 05	0.016 30	0.015 06	0.014 77
7	0.035 41	0.020 24	0.018 82	0.017 80
8	0.041 47	0.038 51	0.037 83	0.037 25

(iii) the temperature profiles do not exhibit the abrupt change in behaviour seen in figures 2(b) and 3(b).

In this regime, the extent and rate of reaction is dependent on power and hot-spot size. In table 2, the depth of burning, r_b , is given for r_0 between 4 and 0.01 m as the power was varied between 4 and 8 W, where r_b measures the position of the midpoint ($x = 0.5$) of the reactant profile at time $t = 200$ min.

At fixed r_0 , we find that r_b increases significantly after $P = 5$ W, although, if we examined the solution profiles at different times, it would be evident that there is no qualitative change in the type of combustion. In all cases, burning is almost complete by $P = 8$ W, and as we increase r_0 we need to slightly decrease the power to obtain this state.

The further we increase N , the more difficult it becomes to achieve complete burning at fixed values of r_0 , commensurate with a restriction on oxygen diffusion. However, at around $N = 8$ we find an additional behaviour for large powers, an example of which is shown in figure 5. In figure 5(b), the reactant is completely burnt in the range $0.016 < r < 0.02$ but only partially burnt in $0.004 < r < 0.016$ when $t = 120$ min. A large power seems to cause quick burning of the solid and complete depletion of the oxygen around the hot-spot in the initial stages. Since the diffusion coefficient of oxygen D_Y is relatively low due to our choice of N , the oxygen cannot reach the partially burnt solid to complete the burning, and therefore the combustion front advances toward the unreacted oxygen. It further seems that somewhere around $t = 120$ min a balance is reached whereby the combustion front cannot advance further due to the cool boundary at $r = r_1$. At this time, the consumption of oxygen in the vicinity of the combustion front slows down sufficiently to allow the oxygen to diffuse back to the hot-spot boundary, allowing complete combustion of the partially burnt solid between r_0 and the front. Table 3 shows the depth of burning r_b for various hot-spot sizes as P is varied between 6 and 24 W. Here, r_b measures the position of $x = 0.5$ at time $t = 200$ min. The value of r_b seems to be insensitive to the hot-spot size and complete burning is only possible for very large values of P . However, for reasonable values of P (around 10 W) we find that approximately half of the solid (a significant portion) is burnt.

One final note is that the calculations revealed a continuum of wave velocities from that determined only by the solid reaction ($N = 0$) to that which is strongly limited by oxygen availability ($N \rightarrow 1$). These velocities are difficult to quantify precisely, but the calculations indicate that the combustion wave velocity is reduced by the restriction of oxygen supply.

3.3. On the effect of the thermal conductivity and the density of the solid

In many of the potential applications of this work, the solid is a particulate material with a relatively low density. Sawdust, for example, has a density of around 270 kg m^{-3} , and we have, therefore, performed some calculations for this value of solid density. In using this value of density, it is necessary to change the value of $\beta = \rho/Y_a$ to around $\beta = 1000$. Figure 6 shows the critical power curve for the aforementioned values (with all other quantities as before) with

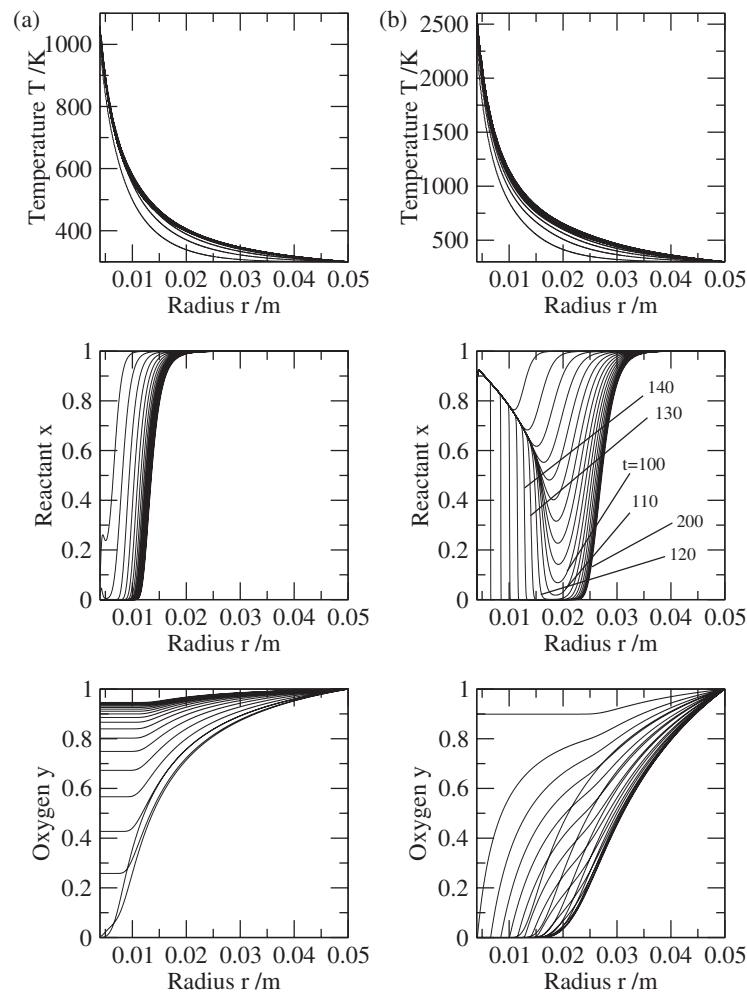


Figure 5. Solution up to $t = 200$ min in steps of 10 min for (a) $P = 4$ W and (b) $P = 12$ W when $N = 10$ and $r_0 = 0.004$ m.

Table 3. The depth of burnt product r_b in metre for $N = 10$ when the hot-spot radius is varied.

Power (W)	$r_0 = 0.01$ m	$r_0 = 0.008$ m	$r_0 = 0.006$ m	$r_0 = 0.004$ m
6	0.018 23	0.018 57	0.018 54	0.018 52
12	0.027 01	0.027 46	0.027 39	0.027 38
18	0.032 98	0.033 09	0.033 10	0.033 10
24	0.035 35	0.035 57	0.035 57	0.035 57

$N = 0.1$. Comparing this curve with the curves in figure 1, it is seen that the basic ‘Z-shape’ (for small enough values of N on the latter) is preserved. However, there are some differences that could be of importance. Comparing figure 6 with the corresponding ($N = 0.1$) curve on figure 1, we see that ‘switch-off’ behaviour (multiple critical powers) occurs at larger values of hot-spot radius. The other difference is that the size of the power required to switch off the

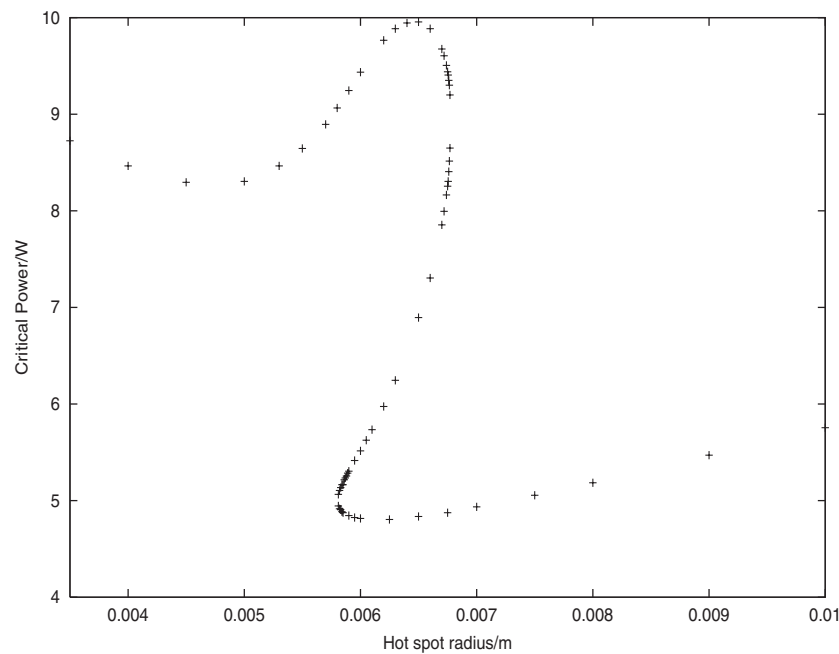


Figure 6. The critical power curve for $N = 0.1$, with $\lambda = 0.1 \text{ W m}^{-1} \text{ K}^{-1}$, $\beta = 1000$ and $\rho = 270 \text{ kg m}^{-3}$. Compare this curve with the $N = 0.1$ ('x') curve in figure 1, where $\rho = 660 \text{ kg m}^{-3}$, $\beta = 2440$ and $\lambda = 0.1 \text{ W m}^{-1} \text{ K}^{-1}$.

combustion wave and to switch it back on is greater; that is, the upper two branches of the curve are higher in figure 6.

The thermal conductivity of the solid can be determined by its packing density. To gain some idea of the effect of the packing density on the ignition behaviour we have also performed some calculations for $\lambda = 0.01 \text{ W m}^{-1} \text{ K}^{-1}$, while keeping $\beta = 2440$ (and therefore $\rho = 660 \text{ kg m}^{-3}$), again with $N = 0.1$. The critical power curve for these values is shown in figure 7. In contrast to figure 6, we find that the switch-off behaviour now occurs at smaller hot-spot sizes and, in general, combustion waves are initiated at much lower values of power than for $\lambda = 0.1 \text{ W m}^{-1} \text{ K}^{-1}$. From the work in [8], the lower branch of the critical curve can be approximated by the formula $P = 4\pi r_0 \lambda Q / C_p$, which is consistent with figure 7, where we find that lowering the value of λ by a factor of 10 lowers the critical power by the same order of magnitude.

4. Experimental validation

The direct comparison with practical circumstances involves very small power sources, as might occur at a kink in a damaged power cable buried within a combustible material. Typically, this might be a wood sawdust insulation layer, or a product that inadvertently accumulates in a crevice of a processing plant where electricity cables are located. In many cases, there are likely to be additional chemical complexities associated, such as the evolution of gaseous products and even void creation around the source when the combustion takes place. These are issues to be addressed in subsequent work.

As a forerunner, our concern is to seek validation of this model. To do so we turn to laboratory experiments [13] that involve a small power source (0.05 m) embedded in a

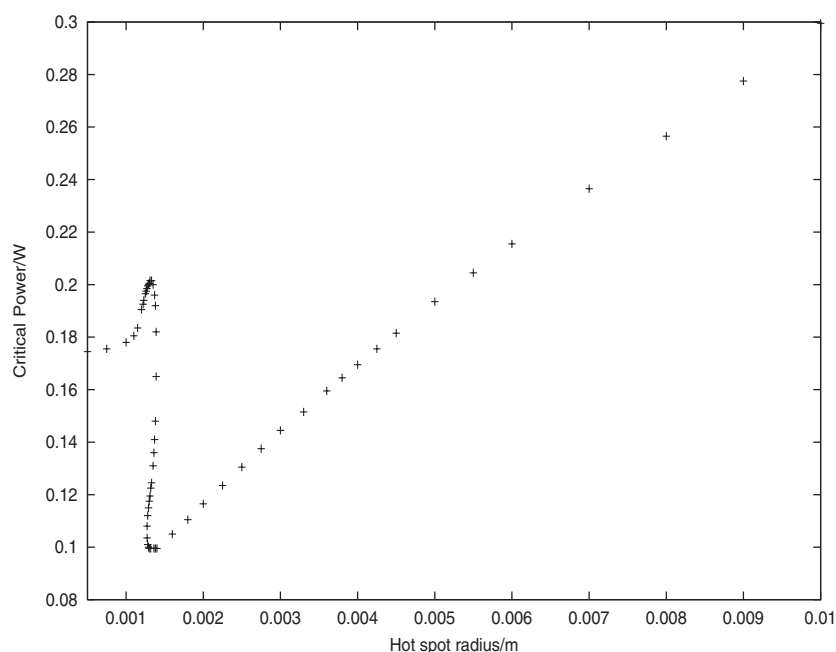
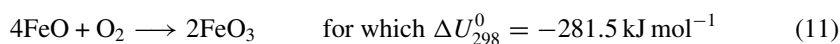


Figure 7. The critical power curve for $N = 0.1$, with $\lambda = 0.01 \text{ W m}^{-1} \text{ K}^{-1}$, $\beta = 2440$ and $\rho = 660 \text{ kg m}^{-3}$. Compare this curve with the $N = 0.1$ ('x') curve in figure 1, where $\rho = 660 \text{ kg m}^{-3}$, $\beta = 2440$ and $\lambda = 0.1 \text{ W m}^{-1} \text{ K}^{-1}$.

cube of particulate reactive material (side-length 0.05, 0.1 and 0.2 m), packed to a density of 660 kg m^{-3} . The process taking place is the oxidation of iron (II) oxide, which may be represented by



and for which the only gas movement is the diffusion of oxygen into the system. The critical power required from a 0.005 m source was not easy to obtain with high precision in this system, but it fell reproducibly in the range 3–4 W, with little dependence on cube size. This critical power is consistent with the predictions at very low values of N , for which oxygen diffusion is not rate controlling, and is an important datum point. More densely packed materials would adversely affect the ingress of oxygen.

From thermocouple experiments within the material in the 0.05 m basket, located at approximately half distance between the source surface and the outer edge, a constant temperature of about 650 K was established after approximately 1 h. This followed an overshoot, reaching a maximum of about 800 K as a result of exothermic oxidation. These times are comparable with the numerical results which show that the time to ignition increases to hours for larger values of the ratio N (restricted oxygen supply), but the temperatures are somewhat lower than that predicted by the numerical results.

5. Scaling

The prediction of ignition is not restricted to small sizes. In non-dimensional terms, the beginning of ignition represented by the left-hand cusp of the Z-shaped curve illustrated in

figure 1 occurs at the following values [1] of re-normalized radius ξ_0^* and power α^* :

$$\xi_0^* \equiv \xi_0 \sqrt{a} = \frac{r_0}{\sqrt{\lambda/\rho c_p A Y_a}} \approx 2 \times 10^{-3}, \quad \alpha^* \equiv \frac{\alpha}{\sqrt{a}} = \frac{P R \sqrt{\lambda/\rho c_p A Y_a}}{4\pi r_0^2 \lambda E} \approx 3 \times 10^{-3}, \quad (12)$$

where $QR/c_p E = 0.075$. Hence, for example, with λ , ρ and c_p the same, to achieve the same cusp in (ξ_0^*, α^*) space, with an increased size hot-spot, $(AY_a)^2$ would have to be decreased by the same amount, thus keeping $r_0 \sqrt{AY_a}$ the same. Hence, the onset of the subtle switch-on and switch-off ignition behaviour implied by figure 1 at about 0.003 m hot-spot (using the data of table 1) would still occur for a 0.03 m hot-spot, if the material was 300 times less reactive, that is, if AY_a was $1 \times 10^{-3} \text{ s}^{-1}$. For a similar critical power level then $(P/\sqrt{AY_a} r_0^2 E)$ would need to remain the same, that is, $P/(r_0 E)$. Thus, a lower activation energy would still yield a similar critical power for a larger hot-spot. To keep $QR/c_p E = 0.075$, the heat release Q would need then to reduce in proportion.

6. Conclusions and future development

We have shown here that when the reaction depends on the supply of oxygen a hot-spot can still be the cause of a self-propagating combustion front. As the supply of oxygen becomes more restricted, it becomes more difficult to initiate self-sustaining combustion waves, and this mode eventually ceases to exist. Nevertheless, even with severe oxygen limitation at fixed r_0 , complete burning of the solid is possible for increasingly larger powers. For realistic values of oxygen supply we have shown that a Z-shaped critical power versus hot-spot radius relationship is observed.

The Z-shaped critical curve that we find for small N is due to the three-dimensional nature of the geometry. This was shown in an earlier work [1] and this behaviour does not occur for the slab and cylindrical geometries, as demonstrated in [3].

Further progress can be made by either allowing the hot-spot boundary to move or taking into account the void created by reactant depletion around the hot-spot. In this paper, it was assumed that the product of reaction was itself a solid with properties identical to that of the reactant. Future work will seek to address reactions in which the product is a gas. This can happen if, for example, the solid is char, in which case one could have a reaction of the type carbon + oxygen \rightarrow carbon dioxide. In this case, it is necessary to consider the fuller problem, that is, the coupling of reaction–diffusion with gas dynamics in a porous reacting solid. Another route worth investigating is that of sequential reactions in which the reactant burns to form a char, which subsequently reacts to form gaseous products. Finally, it will be important to extend this work to more complex geometries such as any three-dimensional shape in which the hot-spot is asymmetrically located.

Acknowledgments

The authors are grateful to the EPSRC for financial support through Research Grant GR/R 22179.

References

- [1] Brindley J, Griffiths J F and McIntosh A C 2001 Ignition phenomenology and criteria associated with hotspots embedded in a reactive material *Chem. Eng. Sci.* **56** 2037–46

- [2] Brindley J, Griffiths J F and McIntosh A C 2001 Potential hazards from spherical hotspots in reactive solids *Proc. 3rd International Seminar on Fire and Explosion Hazards* ed Bradley *et al*
- [3] Brindley J, Griffiths J F, McIntosh A C and Zhang J 2001 Initiation of combustion waves in solids and the effect of geometry *ANZIAM J.* **43** 149–63
- [4] Gray B F and Wake G C 1993 Initial conditions for thermal ignition *Math. Comput. Modelling* **18** 65–75
- [5] Gray B F and Kordylewski W 1988 Travelling waves in exothermic systems *Proc. R. Soc. A* **416** 103–13
- [6] Kapila A K 1981 Evolution of a deflagration in a cold combustible subjected to a uniform energy flux *Int. J. Eng. Sci.* **19m** 495–509
- [7] Linan A and Williams F A 1971 Theory of ignition of a reactive solid by constant energy flux *Combust. Sci. Technol.* **3** 91–8
- [8] McIntosh A C, Brindley J and Griffiths J F An approximate model for the ignition of reactive materials by a hot-spot with reactant depletion *Math. Comput. Modelling* Special volume to mark the retirement of Professor J Brindley, at press
- [9] Mercer G N, Weber R O, Gray B F and Watt S D 1996 Combustion pseudo-waves *Math. Comput. Modelling* **24** 29–38
- [10] Mercer G N, Weber R O and Sidhu H S 1999 An oscillatory route to extinction for solid fuel combustion waves due to heat losses *Proc. R. Soc. A* **454** 2015–22
- [11] Vazquez-Espi C and Linan A 2002 Thermal-diffusive ignition and flame initiation by a local energy source *Combust. Theory Modelling* **6** 297–315
- [12] Watt S D, Weber R O, Sidhu H S and Mercer G N 1999 A weight-function approach for determining watershed initial conditions for combustion zones *IMA J. Appl. Math.* **62** 195–206
- [13] Nelson M, Hazard-Assessment Section, Zeneca Fine Chemicals, unpublished results